Spin-Controlled Quantum Interference of Levitated Nanorotors

Cosimo C. Rusconi,[1,2] Maxime Perdriat,[3] Gabriel Hétet,[3] Oriol Romero-Isart,[4,5] and Benjamin A. Stickler[6]
[1]Max-Planck-Institut für Quantenoptik, Hans-Kopfermann-Strasse 1, 85748 Garching, Germany
[2]Munich Center for Quantum Science and Technology, Schellingstrasse 4, D-80799 München, Germany
[3]Laboratoire De Physique de l'École Normale Supérieure, École Normale Supérieure, PSL Research University, CNRS, Sorbonne Université, Université de Paris, 24 rue Lhomond, 75231 Paris Cedex 05, France
[4]Institute for Quantum Optics and Quantum Information of the Austrian Academy of Sciences, 6020 Innsbruck, Austria
[5]Institute for Theoretical Physics, University of Innsbruck, 6020 Innsbruck, Austria
[6]Faculty of Physics, University of Duisburg-Essen, Lotharstraße 1, 47057 Duisburg, Germany

(Received 22 March 2022; accepted 18 July 2022; published 25 August 2022)

We describe how to prepare an electrically levitated nanodiamond in a superposition of orientations via microwave driving of a single embedded nitrogen-vacancy (NV) center. Suitably aligning the magnetic field with the NV center can serve to reach the regime of ultrastrong coupling between the NV and the diamond rotation, enabling single-spin control of the particle's three-dimensional orientation. We derive the effective spin-oscillator Hamiltonian for small amplitude rotation about the equilibrium configuration and develop a protocol to create and observe quantum superpositions of the particle orientation. We discuss the impact of decoherence and argue that our proposal can be realistically implemented with near-future technology.

DOI: 10.1103/PhysRevLett.129.093605

Levitated dielectric nanoparticles have been recently cooled to their motional ground state [1–3]. This paves the way to realize some of the formidable promises for fundamental and applied science held by massive systems in the quantum regime [4–8]. While in the first ground-state-cooling experiments, the center-of-mass motion of the optically trapped particles is Gaussian [9], the observation of quantum interference requires generating non-Gaussian states of motion [10]. Achieving such states requires a nonlinearity—for instance in the form of a nonlinear external potential [11], or by coupling the mechanical system to a nonlinear system. In the context of spin mechanics—the coupled dynamics of spin and mechanical motion—the nonlinearity is provided by the spin degree of freedom in, for instance, few electrons in solid state defects [12–19], superconducting qubits [20–24], or electronic states of atoms [25–27]. Coherent spin-mechanical interfaces are, however, hard to realize as the coupling between the spin and a mechanical oscillator is usually smaller than the characteristic frequencies of the two systems, as well as their typical decoherence rates [18,28].

In levitated systems, much attention has been devoted to the coupling between internal spins and the center-of-mass motion [14,16,29–33], and more recently the rotational motion of the hosting particle [7,34,35]. The fact that both magnetization and mechanical rotation contribute to the angular momentum of the body provides new and largely unexplored means of spin-rotational coupling [35–37]. In particular, in the presence of an applied magnetic field the librations—small oscillations in the particle orientation around a fixed configuration—of an electrically levitated diamond couple to the spin of embedded nitrogen-vacancy (NV) centers [38]. Such spin-libration coupling has the potential for reaching the strong coupling regime [38,39], as highlighted by recent experimental progress [40–42]. These approaches, however, require one to either carefully select the particle shape [38] or to exploit the collective coupling to many spins [39,42] at the cost of losing the desired nonlinearity.

In this Letter, we theoretically show how it is possible to achieve the so-called single-spin ultrastrong coupling (USC) regime [43], where the coupling between a *single* NV spin and the libration of a levitated diamond is even larger than the characteristic frequencies of both the libration and the spin degrees of freedom. We argue that this can be experimentally implemented with only minor modifications of existing experimental setups [38,42]. In addition, we propose a protocol that uses such large spin-libration coupling to prepare and read out the diamond in a superposition of its orientation.

We consider a homogeneously charged symmetric diamond, modeled as a prolate spheroid with major (minor) semiaxis length a (b), levitated in a ring Paul trap [44]; see

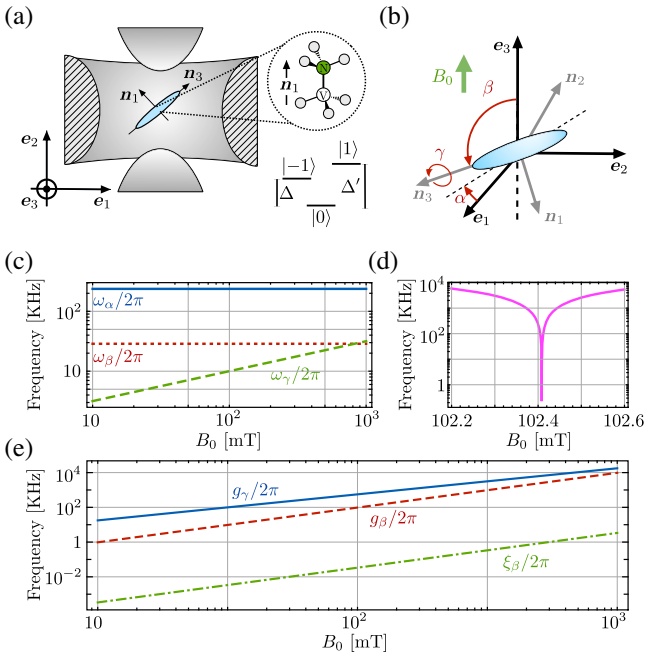

FIG. 1. (a) A charged spheroidal-shaped particle with embedded NV center, whose axis is aligned with body-frame direction $\boldsymbol{n}_1$ perpendicular to the symmetry axis $\boldsymbol{n}_3$, is levitated in a ring-shaped Paul trap. The levels $|\pm 1\rangle$ are split by the applied field B_0. (b) The rotor performs small libration oscillations about the equilibrium orientation in the trap. (c) Characteristic mechanical libration frequency of the rotor as function of the applied field. (d) Frequency Δ of the transition $|0\rangle \leftrightarrow |-1\rangle$ (qubit splitting) close to the ground state level anticrossing, $B_0 \approx 102.4$ mT. (e) Spin-mechanical coupling as function of the applied field. For $a = 100$ nm, $b = a/5$, mass density $\rho_M = 3.5 \times 10^3$ Kg/m^3, $\varepsilon = 10^{-2}$, $\delta = 0.1$, $U_{\rm dc}/U_{\rm ac} = 5 \times 10^{-3}$, $\omega_0/2\pi = 5$ MHz and gyromagnetic ratio $\gamma_e = 1.76 \times 10^{11}$ rad/Ts.

Figs. 1(a) and 1(b). The diamond hosts a single NV center with spin angular momentum $\hat{\boldsymbol{S}}$ and spin quantization axis aligned orthogonal to the particle symmetry axis. The Paul trap creates a confining potential for both the particle center of mass and orientation [38,45]. For a uniformly charged spheroid the center-of-mass and rotational dynamics are decoupled. The spin-rotational dynamics of the system can then be described by

$$\hat{H}(t) = \frac{\hbar^2}{2I}[(\hat{J}_1 - \hat{S}_1)^2 + (\hat{J}_2 - \hat{S}_2)^2] + \frac{\hbar^2}{2I_3}(\hat{J}_3 - \hat{S}_3)^2 + \hbar D_{\rm nv}\hat{S}_1^2 + \hbar\omega_L \boldsymbol{e}_3 \cdot \hat{\boldsymbol{S}} + \hat{V}(t), \quad (1)$$

where $\hbar\hat{\boldsymbol{J}}$ denotes the total angular momentum vector operator of the particle. The first line of Eq. (1) is its rotational energy where $\hbar\hat{J}_i - \hbar\hat{S}_i$ is the mechanical angular momentum along the rigid rotor's principal axis $\boldsymbol{n}_i = \boldsymbol{n}_i(\Omega)$ $(i = 1, 2, 3)$, which is related to the laboratory-fixed axis $\boldsymbol{e}_i$ via the three Euler angles $\Omega = \{\alpha, \beta, \gamma\}$ [46]. The two distinct inertia moments of the spheroid are denoted by I and I_3 for rotations orthogonal to and around the symmetry axis, respectively. We choose $\boldsymbol{n}_1$ along the NV axis, while $\boldsymbol{n}_3$ is the particle symmetry axis. The NV ground state spin triplet along the quantisation axis $\boldsymbol{n}_1$ is denoted by $\{|0\rangle, |\pm 1\rangle\}$. The first and second terms on the second line of the Eq. (1) Hamiltonian represent respectively the spin zero-field splitting of frequency $D_{\rm nv} \simeq 2\pi \times 2.87$ GHz and the Larmor precession of the spin in the external magnetic field, aligned with the space fixed $\boldsymbol{e}_3$ axis, where $\omega_L \equiv \gamma_{\rm nv} B_0/\hbar$ and $\gamma_{\rm nv} > 0$ is the NV gyromagnetic ratio. The mechanical rotation and the internal spin are coupled by two different mechanisms. The first one is the Barnett and Einstein–de Haas effect represented by terms of the form $\hat{J}_i\hat{S}_i/I_i$. The second coupling arises from the interaction between the spin and the applied field, as $\boldsymbol{e}_3 \cdot \hat{\boldsymbol{S}} = -\hat{S}_1 \cos\hat{\gamma}\sin\hat{\beta} + \hat{S}_2 \sin\hat{\gamma}\sin\hat{\beta} + \hat{S}_3\cos\hat{\beta}$, and it can be tuned via the external field [38,40], where $\hat{\alpha}$, $\hat{\beta}$, and $\hat{\gamma}$ are the Euler angle operators. This latter coupling mechanism produces a spin-dependent potential for the rotation of the particle about its symmetry axis. The last term in Eq. (1) is the time-dependent Paul trap potential for the rotational motion,

$$\hat{V}(t) \equiv \frac{3U(t)\Delta Q}{2\ell_0^2}\left[\left(1 + \frac{\delta}{3}\right)\sin^2\hat{\alpha} - \frac{2\delta}{3}\right]\sin^2\hat{\beta}, \quad (2)$$

where $U(t) = U_{\rm dc} + U_{\rm ac}\cos(\omega_0 t)$ is the applied voltage generating the quadrupole electric field [55], $\omega_0/2\pi$ the ac voltage frequency, $\Delta Q/q \simeq (a^2 + 2b^2)/4$ for $b \ll a$ is the quadrupole anisotropy of the particle, q is its total charge, ℓ_0 the characteristic length scale of the trap, and the asymmetry parameter $0 \le \delta < 1$ characterizes deviations from the cylindrical symmetry of the Paul trap. We note that to achieve confinements along both α and β it is necessary for the Paul trap to be asymmetric ($\delta \neq 0$).

A stable solution of Eq. (1) corresponds to $\boldsymbol{n}_3 \| \boldsymbol{e}_1$, spin in $|-1\rangle$ and $\boldsymbol{n}_1$ antiparallel to $\boldsymbol{e}_3$, that is the spin quantization axis antialigned along the external B field [56]. In this regime, the particle performs small oscillations (librations) around the equilibrium orientation ($\alpha = 0$, $\beta = \pi/2$, and $\gamma = \pi$). When $\varepsilon \equiv U_{\rm ac}\Delta Q/(I\omega_0^2\ell_0^2) \ll 1$ and $U_{\rm dc}/U_{\rm ac} \ll 1$ [57], the libration dynamics has two distinct contributions, a fast small amplitude micromotion on top of a slowly evolving large amplitude macromotion (secular dynamics) [45,49,58]. In this regime, it is possible to derive a Hamiltonian describing the coherent interaction between the NV center and the secular harmonic fluctuation of the rotor's orientation about the equilibrium. This is done in three steps. First, we derive the secular Hamiltonian of the system [46]. Second, we expand the secular Hamiltonian about the equilibrium solution up to second order in the libration degrees of freedom. Third, we eliminate $|1\rangle$ by

projecting the spin subsystem on the subspace $\{|0\rangle, |-1\rangle\} \equiv \{|\downarrow\rangle, |\uparrow\rangle\}$. We will consider values of the magnetic field larger than 10 mT for which $|1\rangle$ is far detuned from the remaining degrees of freedom. At the end of these steps, $\hat{\alpha}$ decouples from the remaining degrees of freedom, whose dynamics are described by the following qubit-oscillator Hamiltonian:

$$\hat{H} = \frac{\hbar\Delta}{2}\hat{\sigma}^z + \frac{\hat{p}_\beta^2}{2I} + \frac{I}{2}\omega_\beta^2\hat{\beta}^2 + \frac{\hat{p}_\gamma^2}{2I_3} + \frac{I_3}{2}\omega_\gamma^2\left(\frac{\mathbb{1}+\hat{\sigma}^z}{2}\right)\hat{\gamma}^2 - \hbar g_\gamma\frac{\hat{\gamma}}{\gamma_0}\hat{\sigma}^x - \hbar g_\beta\frac{\hat{\beta}}{\beta_0}\hat{\sigma}^y + \hbar\xi_\beta\left(\frac{\hat{\beta}}{\beta_0}\right)^2\hat{\sigma}^z. \tag{3}$$

Here, we defined the qubit splitting $\Delta \equiv D_{\rm nv} - \omega_L$, the libration frequencies $\omega_\beta \equiv \omega_0[2\delta\varepsilon U_{\rm dc}/U_{\rm ac} + 2\delta^2\varepsilon^2]^{1/2}$, $\omega_\gamma \equiv (\hbar\omega_L/I_3)^{1/2}$, and the coupling rates $g_\gamma \equiv \omega_L\gamma_0/\sqrt{2}$, $g_\beta \equiv \omega_L\beta_0/\sqrt{2}$, and $\xi_\beta \equiv \omega_L\beta_0^2/2$ with the zero-point amplitudes $\beta_0 \equiv \sqrt{\hbar/2I\omega_\beta}$, $\gamma_0 \equiv (\hbar/\sqrt{2}I_3\omega_\gamma)^{1/2}$. The dynamics of $\hat{\alpha}$ undergoes harmonic oscillations at the frequency $\omega_\alpha \equiv \omega_0\{(1+\delta/3)[3\varepsilon U_{\rm dc}/U_{\rm ac} + 9\delta^2\varepsilon^2/2]\}^{1/2}$. We neglected the Barnett and Einstein-de Haas coupling terms in Eq. (3), because in the libration regime they give a negligible contribution as compared to the coupling between the spin and the magnetic field. Figures 1(c)–1(e) show the frequencies and coupling rates appearing in Eq. (3) as a function of the applied magnetic field B_0 and for $a = 100$ nm and $a/b = 5$. Importantly, the system is in the USC regime as $g_\gamma \gg \omega_\gamma$ and $g_\beta \gg \omega_\beta$ [cf. Figs. 1(c) and 1(e)].

Let us now focus on the dispersive regime of qubit-oscillator interaction, i.e., when $|\Delta| \gg g_\gamma, g_\beta$. In this case, mechanically induced spin transitions are suppressed and the coupling induces a spin-dependent shift of the oscillator frequencies. As a consequence of the USC in Eq. (3), these shifts can be exploited to prepare a non-Gaussian state of the $\hat{\gamma}$ degree of freedom. In the dispersive limit, the effective dynamics of the system is diagonal in the eigenbasis of $\hat{\sigma}^z$, and described by [46]

$$\hat{H}' = \left(\hat{H}_\uparrow + \frac{\hbar\Delta}{2}\right)\otimes|\uparrow\rangle\langle\uparrow| + \left(\hat{H}_\downarrow - \frac{\hbar\Delta}{2}\right)\otimes|\downarrow\rangle\langle\downarrow|, \tag{4a}$$

where $\hat{H}_{\uparrow\downarrow}$ depends on the sign of Δ. For $\Delta > 0$, they read

$$\frac{\hat{H}_\uparrow}{\hbar} \equiv \tilde{\omega}_\beta\hat{b}^\dagger\hat{b} + \tilde{\omega}_\gamma\hat{c}^\dagger\hat{c}, \tag{4b}$$

$$\frac{\hat{H}_\downarrow}{\hbar} \equiv \tilde{\omega}_\beta\hat{b}^\dagger\hat{b} - \frac{\chi_\beta}{2}(\hat{b}+\hat{b}^\dagger)^2 + \tilde{\omega}_\gamma\hat{c}^\dagger\hat{c} - \frac{\chi_\gamma}{2}(\hat{c}^\dagger+\hat{c})^2. \tag{4c}$$

Here, we introduced the bosonic operators $\hat{c}$ and $\hat{b}$ according to $\hat{\beta} \equiv \beta_0(\hat{b}^\dagger + \hat{b})$ and $\hat{\gamma} \equiv \sqrt{\hbar/2I_3\tilde{\omega}_\gamma}(\hat{c}^\dagger + \hat{c})$, and the oscillator frequencies $\tilde{\omega}_\beta \equiv [\omega_\beta^2 + \hbar\omega_L(1+\omega_L/\Delta)/I]^{1/2}$, $\chi_\beta \equiv \hbar\omega_L(1+\omega_L/\Delta)/(I\tilde{\omega}_\beta)$, $\tilde{\omega}_\gamma \equiv [\hbar\omega_L(1+\omega_L/\Delta)/I_3]^{1/2}$, and $\chi_\gamma \equiv \hbar\omega_L(1+2\omega_L/\Delta)/(2I_3\tilde{\omega}_\gamma)$. Aside from a small region around $B_0 = 102.4$ mT where $\Delta = 0$, the qubit splitting always satisfies the dispersive regime conditions [cf. Figs. 1(d) and 1(e)] (see also Ref. [46]). Equation (4a) describes a spin-dependent evolution of the β and γ libration modes [59]. On the other hand, the dynamics of $\hat{\gamma}$ changes between an attractive potential in Eq. (4b) to a repulsive potential in Eq. (4c) depending on the spin state, since $2\chi_\gamma > \tilde{\omega}_\gamma$. The appearance of a repulsive potential for $|\downarrow\rangle$ is a consequence of the large dispersive shift in the USC regime. We remark that the following protocol does not require the use of the quartic term $\hat{\gamma}^4$ that is also found in the dispersive regime [60].

Let us assume that the total system is initially uncorrelated, $\rho = \rho_{\rm th} \otimes |\uparrow\rangle\langle\uparrow|$, where $\rho_{\rm th}$ is the thermal state of Eq. (4b). The protocol consists of the following three steps [see Figs. 2(a) and 2(b)]. (i) Apply a $\pi/2$-microwave pulse preparing the state $\hat{\rho}_1 = \hat{\rho}_{\rm th} \otimes (|\uparrow\rangle\langle\uparrow| + |\downarrow\rangle\langle\uparrow| + |\uparrow\rangle\langle\downarrow| + |\downarrow\rangle\langle\downarrow|)/2$ and let it evolve for a time τ. (ii) Apply a π-microwave pulse such that $|\uparrow(\downarrow)\rangle \to |\downarrow(\uparrow)\rangle$ and let the system evolve for another time τ. (iii) Apply a $\pi/2$-microwave pulse such that $|\uparrow(\downarrow)\rangle \to (|\uparrow\rangle \pm |\downarrow\rangle)/\sqrt{2}$ and perform a spin measurement in the basis $\{|\uparrow\rangle, |\downarrow\rangle\}$. This yields the qubit in the state $|\uparrow(\downarrow)\rangle$ with probability [46]

$$P_{\uparrow\downarrow}(\tau) = \frac{1}{2} \pm \frac{e^{-2\Gamma_2\tau}}{2}{\rm Re}({\rm Tr}[\hat{U}_\downarrow^\dagger\hat{U}_\uparrow^\dagger\hat{U}_\downarrow\hat{U}_\uparrow\rho_{\rm th}]), \tag{5}$$

where $\hat{U}_{\uparrow\downarrow} \equiv \exp(-i\tau\hat{H}_{\uparrow\downarrow}/\hbar)$. The total duration of the protocol is 2τ. We neglected the evolution of the oscillator during the microwave pulses as these are typically much shorter than the mechanical period. In Eq. (5) we included the effect of qubit dephasing at a rate $\Gamma_2 = 2\pi/T_2$, which acts during steps (i) and (ii) while the spin state is in a superposition, assuming a Markovian dephasing process [61]. Observing revivals in the final probability Eq. (5) as a function of the duration τ of steps (i) and (ii) is sufficient to conclude that the oscillators were in a coherent superposition state during the evolution [63–65]. The protocol can be interpreted as follows. After the first microwave $\pi/2$ pulse, the state of the particle evolves in an entangled state of the spin-oscillator system where the oscillator is in a squeezed thermal state and in the initial thermal state for a spin in $|\downarrow\rangle$ and $|\uparrow\rangle$, respectively [see central panel in Fig. 2(b)]. The π pulse reverses the role of the spin. The oscillator's state corresponding to a spin in $|\uparrow\rangle$ is in a squeezed state and rotates in phase space at the rate $\tilde{\omega}_\gamma$ according to $\hat{H}_\uparrow$. At the same time the oscillator state corresponding to $|\downarrow\rangle$ evolves from a thermal state to a squeezed thermal state [right panel in Fig. 2(b)]. The second $\pi/2$ pulse in step (iii) brings the two branches

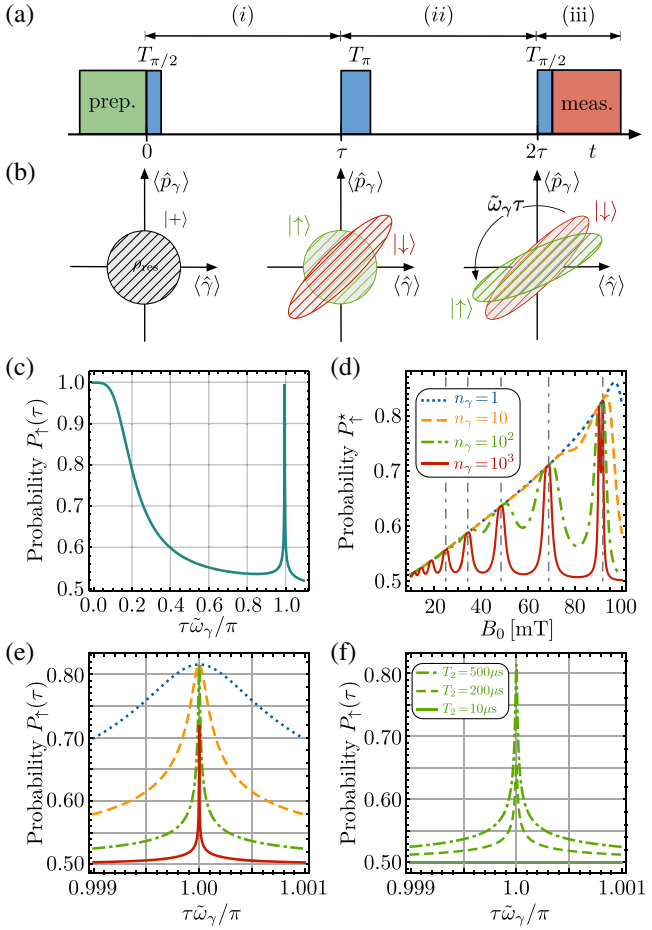

FIG. 2. (a) Pulse sequence for the spin control during the protocol and corresponding steps (i–iii). (b) Oscillator's state at different steps of the protocol: initial thermal state (left panel), at the end of step (i) (middle panel), and at the end of step (ii) (right panel). Note that the state corresponding to $|\uparrow\rangle(|\downarrow\rangle)$ is always represented in green (red), while the π pulse reverses the spin state between the middle and right panel. The rightmost panel shows that for $\tau = \pi/\tilde{\omega}_\gamma$ the two squeezed states overlap perfectly. (c) Probability $P_\uparrow(\tau)$ as a function of τ in the absence of dephasing ($\Gamma_2 = 0$), for $n_{\rm th} = 1$ and for negligible coupling to the β mode. (d) $P^\star_\uparrow$ as a function of B_0 for $T_2 = 0.5$ ms and for different initial thermal occupation n_γ (see legend), assuming that β has the same initial temperature [46]. The maxima occur at those values of B_0 where $\tilde{\omega}_\beta/\tilde{\omega}_\gamma = n$. Panels (e) and (f) show $P_\uparrow(\tau)$ around $\tau = \pi/\tilde{\omega}_\gamma$ for $B_0 = 90$ mT, respectively, for different spin initial thermal occupation n_γ at $T_2 = 0.5$ ms and for different dephasing times at $n_\gamma = 100$ as specified in the legend.

together, leading to the interference between the two oscillator states in superposition. At $\tau = \pi/\tilde{\omega}_\gamma$ the states of the two branches overlap perfectly, leading to a rephasing of $P_{\uparrow\downarrow}$ [Fig. 2(c)]. The evolution of the state of the mode β during the protocol is similar [54,66] but with a rephasing time $\pi/\tilde{\omega}_\beta$. When $\tilde{\omega}_\gamma/\tilde{\omega}_\beta = n \in \mathbb{N}$, which occurs at particular B-field values $\tilde{B}_n$, the two modes rephase at the same time, leading to a maximum value for $P^\star_{\uparrow\downarrow} \equiv P_{\uparrow\downarrow}(\pi/\tilde{\omega}_\gamma)$ [Fig. 2(d)] [46]. We note that maxima in $P^\star_\uparrow$ are obtained even if the condition $B_0 = \tilde{B}_n$ is not met exactly. For $B_0 \simeq \tilde{B}_n$, the value of $P^\star_\uparrow$ is robust to the initial thermal occupation of the oscillators, which mostly affects its width [Fig. 2(e)] and is mainly affected by the qubit T_2^* time [Fig. 2(f)]. A superposition state can thus be successfully created also for the oscillator in a highly occupied thermal state as shown in Fig. 2(d). For detecting the rephasing in $P_{\uparrow\downarrow}(\tau)$, it is, however, beneficial to reduce the initial state temperature down to few milli-Kelvin or lower, using for instance recently developed cooling schemes for the rotational motion of levitated particle [41,45,67–70].

We discussed the protocol for the case $\Delta > 0$ in Eq. (4a). For $\Delta < 0$, Eq. (3) leads to trapped dynamics for the qubit in $|\downarrow\rangle$, and to a repulsive potential for both modes for $|\uparrow\rangle$. For the execution of the protocol discussed above, this regime is, however, more susceptible to imperfection as compared to $\Delta > 0$ [46].

The proposed interference protocol enables the preparation of superposition states provided the relevant decoherence rates are smaller than the protocol's duration $2\pi/\tilde{\omega}_\gamma$. The qubit-oscillator system exhibits three main damping mechanisms [39]: (i) scattering of background gas and emission of thermal photons, (ii) electric and magnetic field noise, and (iii) dephasing and damping of the NV spin. The first two can be usually reduced at sufficiently low pressure and temperatures, and by having the trapping region sufficiently distant from the trap electrodes [39,71]. Dephasing of the NV spin poses a stronger requirement on the feasibility of the protocol even at cryogenic temperatures as generally $1/T_2^* \gtrsim \tilde{\omega}_\gamma/2\pi$. Exceptionally long dephasing times, such as $T_2^* \sim 0.5$ ms, which we used in Figs. 2(d) and 2(e), have been reported [72] in isotopically purified diamonds with low ^{13}C concentration [73]. Let us note that our interference protocol may actually dynamically decouple the NV spin prolonging the coherence time to $T_2 > T_2^*$, which is eventually limited to few milliseconds due to irreversible coupling to lattice vibrations. Finally, the visibility of the revival in Eq. (5) is also affected by coupling between the libration and center-of-mass oscillations of the nanodiamond. This originates from a slight asymmetry in the charge distribution that generates a permanent dipole moment of the nanodiamond. This coupling has been estimated in [24] and shown to be negligible for highly charged nanoscale objects. Postselection of the trapped particle could thus be used to reduce this effect. Let us finally note that asymmetry in the particle shape might add a contribution to the trapping potential for γ as shown in [35].

Several of the main ingredients of our proposal have been independently realized. Trapping, controlling, and cooling of the center of mass and libration of diamond particles in a Paul trap has been realized in several

experiments (see Refs. [5,6] and references therein). Selective loading of a particle containing a single NV center in optical and hybrid traps has been reported [17,74–76]. Finally, precise spin initialization and microwave control of NV centers at cryogenic temperature has been demonstrated [77–79]. A recent experiment has also demonstrated the possibility of tuning the libration potential between attractive and repulsive using the coupling to an ensemble of NV in the spin para-diamagnetic regime [42]. While putting all these results together is not a straightforward endeavor, we see no major roadblock in implementing our proposal in the near future.

In conclusion, we have shown that the spin-libration coupling in electrically levitated nanodiamond can realistically reach the single-spin ultrastrong coupling regime, requiring only minor modifications of existing setups [38,40,41]. Furthermore, we have shown how to take advantage of such large nonlinearity to prepare non-Gaussian states of the particle libration. In addition, the ability to create mechanical squeezed states could be useful for the detection of weak forces [66,80,81]. Our Letter thus presents levitated nanodiamonds with embedded spins as a highly attractive system for massive superposition experiments exploiting ultrastrong single spin-mechanical coupling rates.

C. C. R. acknowledges funding from ERC Advanced Grant QUENOCOBA under the EU Horizon 2020 program (Grant Agreement No. 742102). B. A. S. acknowledges support by the Deutsche Forschungsgemeinschaft (DFG, German Research Foundation)—411042854. This work has been supported by Region Île-de-France in the framework of the DIM SIRTEQ.

[1] U. Delić, M. Reisenbauer, K. Dare, D. Grass, V. Vuletić, N. Kiesel, and M. Aspelmeyer, Science **367**, 892 (2020).
[2] L. Magrini, P. Rosenzweig, C. Bach, A. Deutschmann-Olek, S. G. Hofer, S. Hong, N. Kiesel, A. Kugi, and M. Aspelmeyer, Nature (London) **595**, 373 (2021).
[3] F. Tebbenjohanns, M. L. Mattana, M. Rossi, M. Frimmer, and L. Novotny, Nature (London) **595**, 378 (2021).
[4] J. Millen and B. A. Stickler, Contemp. Phys. **61**, 155 (2020).
[5] C. Gonzalez-Ballestero, M. Aspelmeyer, L. Novotny, R. Quidant, and O. Romero-Isart, Science **374**, eabg3027 (2021).
[6] B. A. Stickler, K. Hornberger, and M. S. Kim, Nat. Rev. Phys. **3**, 589 (2021).
[7] M. Perdriat, C. Pellet-Mary, P. Huillery, L. Rondin, and G. Hétet, Micromachines **12**, 651 (2021).
[8] D. C. Moore and A. A. Geraci, Quantum Sci. Technol. **6**, 014008 (2021).
[9] M. Aspelmeyer, T. J. Kippenberg, and F. Marquardt, Rev. Mod. Phys. **86**, 1391 (2014).
[10] O. Romero-Isart, A. C. Pflanzer, M. L. Juan, R. Quidant, N. Kiesel, M. Aspelmeyer, and J. I. Cirac, Phys. Rev. A **83**, 013803 (2011).
[11] J. Bateman, S. Nimmrichter, K. Hornberger, and H. Ulbricht, Nat. Commun. **5**, 4788 (2014).
[12] P. Rabl, P. Cappellaro, M. V. G. Dutt, L. Jiang, J. R. Maze, and M. D. Lukin, Phys. Rev. B **79**, 041302(R) (2009); P. Rabl, S. J. Kolkowitz, F. H. L. Koppens, J. G. E. Harris, P. Zoller, and M. D. Lukin, Nat. Phys. **6**, 602 (2010).
[13] O. Arcizet, V. Jacques, A. Siria, P. Poncharal, P. Vincent, and S. Seidelin, Nat. Phys. **7**, 879 (2011).
[14] M. Scala, M. S. Kim, G. W. Morley, P. F. Barker, and S. Bose, Phys. Rev. Lett. **111**, 180403 (2013).
[15] B. Pigeau, S. Rohr, L. Mercier de Lépinay, A. Gloppe, V. Jacques, and O. Arcizet, Nat. Commun. **6**, 8603 (2015).
[16] C. Wan, M. Scala, S. Bose, A. C. Frangeskou, A. A. Rahman, G. W. Morley, P. F. Barker, and M. S. Kim, Phys. Rev. A **93**, 043852 (2016).
[17] G. P. Conangla, A. W. Schell, R. A. Rica, and R. Quidant, Nano Lett. **18**, 3956 (2018).
[18] J. Gieseler, A. Kabcenell, E. Rosenfeld, J. D. Schaefer, A. Safira, M. J. A. Schuetz, C. Gonzalez-Ballestero, C. C. Rusconi, O. Romero-Isart, and M. D. Lukin, Phys. Rev. Lett. **124**, 163604 (2020).
[19] H. Wang and I. Lekavicius, Appl. Phys. Lett. **117**, 230501 (2020).
[20] A. D. O'Connell, M. Hofheinz, M. Ansmann, R. C. Bialczak, M. Lenander, E. Lucero, M. Neeley, D. Sank, H. Wang, M. Weides, J. Wenner, J. M. Martinis, and A. N. Cleland, Nature (London) **464**, 697 (2010).
[21] O. Romero-Isart, L. Clemente, C. Navau, A. Sanchez, and J. I. Cirac, Phys. Rev. Lett. **109**, 147205 (2012).
[22] G. Via, G. Kirchmair, and O. Romero-Isart, Phys. Rev. Lett. **114**, 143602 (2015).
[23] D. Zoepfl, M. L. Juan, C. M. F. Schneider, and G. Kirchmair, Phys. Rev. Lett. **125**, 023601 (2020).
[24] L. Martinetz, K. Hornberger, J. Millen, M. S. Kim, and B. A. Stickler, npj Quantum Inf. **6**, 101 (2020).
[25] D. Hunger, S. Camerer, M. Korppi, A. Jöckel, T. Hänsch, and P. Treutlein, C. R. Phys. **12**, 871 (2011).
[26] A. C. Pflanzer, O. Romero-Isart, and J. I. Cirac, Phys. Rev. A **88**, 033804 (2013).
[27] T. M. Karg, B. Gouraud, C. T. Ngai, G.-L. Schmid, K. Hammerer, and P. Treutlein, Science **369**, 174 (2020).
[28] T. Oeckinghaus, S. A. Momenzadeh, P. Scheiger, T. Shalomayeva, A. Finkler, D. Dasari, R. Stöhr, and J. Wrachtrup, Nano Lett. **20**, 463 (2020).
[29] Z.-Q. Yin, T. Li, X. Zhang, and L. M. Duan, Phys. Rev. A **88**, 033614 (2013).
[30] S. Bose, A. Mazumdar, G. W. Morley, H. Ulbricht, M. Toroš, M. Paternostro, A. A. Geraci, P. F. Barker, M. Kim, and G. Milburn, Phys. Rev. Lett. **119**, 240401 (2017).
[31] C. Marletto and V. Vedral, Phys. Rev. Lett. **119**, 240402 (2017).
[32] J. S. Pedernales, G. W. Morley, and M. B. Plenio, Phys. Rev. Lett. **125**, 023602 (2020).
[33] Y. Japha and R. Folman, arXiv:2202.10535.
[34] Y. Ma, T. M. Hoang, M. Gong, T. Li, and Z.-q. Yin, Phys. Rev. A **96**, 023827 (2017).
[35] Y. Ma, M. S. Kim, and B. A. Stickler, Phys. Rev. B **104**, 134310 (2021).

[36] C. C. Rusconi and O. Romero-Isart, Phys. Rev. B **93**, 054427 (2016); C. C. Rusconi, V. Pöchhacker, K. Kustura, J. I. Cirac, and O. Romero-Isart, Phys. Rev. Lett. **119**, 167202 (2017); C. C. Rusconi, V. Pöchhacker, J. I. Cirac, and O. Romero-Isart, Phys. Rev. B **96**, 134419 (2017).

[37] T. Sato, T. Kato, D. Oue, and M. Matsuo, arXiv:2202.02461.

[38] T. Delord, L. Nicolas, M. Bodini, and G. Hétet, Appl. Phys. Lett. **111**, 013101 (2017); T. Delord, L. Nicolas, L. Schwab, and G. Hétet, New J. Phys. **19**, 033031 (2017); T. Delord, L. Nicolas, Y. Chassagneux, and G. Hétet, Phys. Rev. A **96**, 063810 (2017).

[39] P. Huillery, T. Delord, L. Nicolas, M. Van Den Bossche, M. Perdriat, and G. Hétet, Phys. Rev. B **101**, 134415 (2020).

[40] T. Delord, P. Huillery, L. Schwab, L. Nicolas, L. Lecordier, and G. Hétet, Phys. Rev. Lett. **121**, 053602 (2018).

[41] T. Delord, P. Huillery, L. Nicolas, and G. Hétet, Nature (London) **580**, 56 (2020).

[42] M. Perdriat, P. Huillery, C. Pellet-Mary, and G. Hétet, Phys. Rev. Lett. **128**, 117203 (2022).

[43] P. Forn-Díaz, L. Lamata, E. Rico, J. Kono, and E. Solano, Rev. Mod. Phys. **91**, 025005 (2019).

[44] W. Paul, Rev. Mod. Phys. **62**, 531 (1990).

[45] L. Martinetz, K. Hornberger, and B. A. Stickler, New J. Phys. **23**, 093001 (2021).

[46] See Supplemental Material at http://link.aps.org/supplemental/10.1103/PhysRevLett.129.093605 for a definition of the convention adopted for rotations, for a derivation of the spin-oscillator Hamiltonian in the dispersive regime, and for additional details on the interference protocol, which includes Refs. [47–54].

[47] C. Gneiting, T. Fischer, and K. Hornberger, Phys. Rev. A **88**, 062117 (2013).

[48] B. S. DeWitt, Phys. Rev. **85**, 653 (1952).

[49] R. J. Cook, D. G. Shankland, and A. L. Wells, Phys. Rev. A **31**, 564 (1985).

[50] C. V. Sukumar and D. M. Brink, Phys. Rev. A **56**, 2451 (1997).

[51] M. Ban, J. Math. Phys. (N.Y.) **33**, 3213 (1992).

[52] D. Martínez-Tibaduiza, A. Aragão, C. Farina, and C. Zarro, Phys. Lett. A **384**, 126937 (2020).

[53] I. S. Gradshteyn and I. M. Ryzhik, *Table of Integrals, Series, and Products*, 5th ed. (Academic Press, New York, 1994).

[54] M. Rashid, T. Tufarelli, J. Bateman, J. Vovrosh, D. Hempston, M. S. Kim, and H. Ulbricht, Phys. Rev. Lett. **117**, 273601 (2016).

[55] Geometrical factors associated with the shape of the electrodes are included in the definition of U_{ac} and U_{dc}.

[56] Note that another stable solution is given by $\boldsymbol{n}_3 \| \boldsymbol{e}_1$, spin in $|1\rangle$ and $\boldsymbol{n}_1$ parallel to $\boldsymbol{e}_3$. Both solutions lead to the same results concerning the spin-oscillator coupling and the interference protocol.

[57] The requirement $U_{\mathrm{dc}}/U_{\mathrm{ac}} \ll 1$ is necessary to guarantee center-of-mass confinement in the Paul trap.

[58] F. G. Major, V. N. Gheorghe, S. P. F. G. Major, G. Werth, G. Werth *et al.*, *Charged Particle Traps: Physics and Techniques of Charged Particle Field Confinement* (Springer Science & Business Media, New York, 2005), Vol. 37.

[59] For values of B_0 such that $\omega_\beta > 2\chi_\beta$, the dynamics of β are harmonic with a frequency determined by the spin state. This requires $B_0 < B^\star$, where $B^\star$ depends on the system parameters. For the parameters considered in Fig. 1, $B^\star \approx 100$ mT. For $B_0 > B^\star$, but still within the dispersive regime, the β potential in Eq. (4c) becomes unstable.

[60] F. Pistolesi, A. N. Cleland, and A. Bachtold, Phys. Rev. X **11**, 031027 (2021).

[61] Decay of free induction decay signal in NV centers has been shown to follow a Gaussian law, $\exp[-(2\tau/T_2^*)^2]$ [62]. For long coherence times such as for isotopically purified diamonds, this leads to a weaker dephasing in our protocol. The assumed exponential decay is thus a worst case scenario.

[62] J. R. Maze, A. Dréau, V. Waselowski, H. Duarte, J.-F. Roch, and V. Jacques, New J. Phys. **14**, 103041 (2012).

[63] S. Bose, K. Jacobs, and P. L. Knight, Phys. Rev. A **59**, 3204 (1999).

[64] F. Marquardt and C. Bruder, Phys. Rev. B **63**, 054514 (2001).

[65] A. D. Armour, M. P. Blencowe, and K. C. Schwab, Phys. Rev. Lett. **88**, 148301 (2002).

[66] F. Cosco, J. S. Pedernales, and M. B. Plenio, Phys. Rev. A **103**, L061501 (2021).

[67] F. van der Laan, R. Reimann, A. Militaru, F. Tebbenjohanns, D. Windey, M. Frimmer, and L. Novotny, Phys. Rev. A **102**, 013505 (2020).

[68] J. Bang, T. Seberson, P. Ju, J. Ahn, Z. Xu, X. Gao, F. Robicheaux, and T. Li, Phys. Rev. Research **2**, 043054 (2020).

[69] F. van der Laan, F. Tebbenjohanns, R. Reimann, J. Vijayan, L. Novotny, and M. Frimmer, Phys. Rev. Lett. **127**, 123605 (2021).

[70] J. Schäfer, H. Rudolph, K. Hornberger, and B. A. Stickler, Phys. Rev. Lett. **126**, 163603 (2021).

[71] K. R. Brown, J. Chiaverini, J. M. Sage, and H. Häffner, Nat. Rev. Mater. **6**, 892 (2021).

[72] P. C. Maurer, G. Kucsko, C. Latta, L. Jiang, N. Y. Yao, S. D. Bennett, F. Pastawski, D. Hunger, N. Chisholm, M. Markham, D. J. Twitchen, J. I. Cirac, and M. D. Lukin, Science **336**, 1283 (2012).

[73] G. Balasubramanian, P. Neumann, D. Twitchen, M. Markham, R. Kolesov, N. Mizuochi, J. Isoya, J. Achard, J. Beck, J. Tissler, V. Jacques, P. R. Hemmer, F. Jelezko, and J. Wrachtrup, Nat. Mater. **8**, 383 (2009).

[74] M. Geiselmann, M. L. Juan, J. Renger, J. M. Say, L. J. Brown, F. J. G. de Abajo, F. Koppens, and R. Quidant, Nat. Nanotechnol. **8**, 175 (2013).

[75] L. P. Neukirch, E. von Haartman, J. M. Rosenholm, and A. Nick Vamivakas, Nat. Photonics **9**, 653 (2015).

[76] G. P. Conangla, R. A. Rica, and R. Quidant, Nano Lett. **20**, 6018 (2020).

[77] L. Robledo, L. Childress, H. Bernien, B. Hensen, P. F. A. Alkemade, and R. Hanson, Nature (London) **477**, 574 (2011).

[78] S. D. Bennett, S. Kolkowitz, Q. P. Unterreithmeier, P. Rabl, A. C. B. Jayich, J. G. E. Harris, and M. D. Lukin, New J. Phys. **14**, 125004 (2012).

[79] D. D. B. Rao, S. A. Momenzadeh, and J. Wrachtrup, Phys. Rev. Lett. **117**, 077203 (2016).

[80] T. Weiss, M. Roda-Llordes, E. Torrontegui, M. Aspelmeyer, and O. Romero-Isart, Phys. Rev. Lett. **127**, 023601 (2021).

[81] K. Kustura, C. Gonzalez-Ballestero, A. d. l. R. Sommer, N. Meyer, R. Quidant, and O. Romero-Isart, Phys. Rev. Lett. **128**, 143601 (2022).